

## STRUCTURE NOTE

# Crystal structure of the N-terminal methyltransferase-like domain of anamorsin

Gaojie Song,<sup>1</sup> Chongyun Cheng,<sup>2,3</sup> Yang Li,<sup>1</sup> Neil Shaw,<sup>1</sup> Zhi-Cheng Xiao,<sup>3\*</sup> and Zhi-Jie Liu<sup>1,2\*</sup>

<sup>1</sup> National Laboratory of Biomacromolecules, Institute of Biophysics, Chinese Academy of Sciences, Beijing 100101, China

<sup>2</sup> iHuman Institute, ShanghaiTech University, Shanghai 200031, China

<sup>3</sup> Department of Anatomy and Developmental Biology, Monash University, Clayton, VIC 3800, Australia

### ABSTRACT

Anamorsin is a recently identified molecule that inhibits apoptosis during hematopoiesis. It contains an N-terminal methyltransferase-like domain and a C-terminal Fe-S cluster motif. Not much is known about the function of the protein. To better understand the function of anamorsin, we have solved the crystal structure of the N-terminal domain at 1.8 Å resolution. Although the overall structure resembles a typical S-adenosylmethionine (SAM) dependent methyltransferase fold, it lacks one  $\alpha$ -helix and one  $\beta$ -strand. As a result, the N-terminal domain as well as the full-length anamorsin did not show S-adenosyl-L-methionine (AdoMet) dependent methyltransferase activity. Structural comparisons with known AdoMet dependent methyltransferases reveals subtle differences in the SAM binding pocket that preclude the N-terminal domain from binding to AdoMet. The N-terminal methyltransferase-like domain of anamorsin probably functions as a structural scaffold to inhibit methyl transfers by out-competing other AdoMet dependant methyltransferases or acts as bait for protein–protein interactions.

Proteins 2013; 00:000–000.  
© 2013 Wiley Periodicals, Inc.

**Key words:** anamorsin; CIAPIN1; crystal structure; methyltransferase-like fold.

### INTRODUCTION

Anamorsin (also called cytokine-induced apoptosis inhibitor 1, CIAPIN1) is a newly identified cytokine induced antiapoptosis molecule that has been shown to play an important role in definitive hematopoiesis in mouse fetal liver.<sup>1</sup> Although anamorsin does not show homology to known apoptosis regulatory molecules, it has been postulated to exert its function by upregulating the expression of Bcl-xL and Jak2. In addition to its protective role against cytokine withdrawal, murine anamorsin has also been shown to protect IL-3-dependent pro-B cell line, Ba/F3, from other apoptotic stimuli such as etoposide,  $\gamma$ -radiation, and staurosporine.<sup>1</sup> Anamorsin

has been studied extensively for its role in development of multidrug resistance. It has been found to be upregulated at both mRNA and protein levels during

Grant sponsor: Ministry of Science and Technology of China; Grant number: 2014CB910400.

Gaojie Song and Chongyun Cheng contributed equally to this work

\*Correspondence to: Zhi-Cheng Xiao, Department of Anatomy and Developmental Biology, Monash University, Clayton, VIC 3800, Australia. E-mail: zhicheng.xiao@monash.edu or Zhi-Jie Liu, National Laboratory of Biomacromolecules, Institute of Biophysics, Chinese Academy of Sciences, Beijing 100101, China. E-mail: zjliu@ibp.ac.cn

Received 19 August 2013; Revised 19 September 2013; Accepted 26 September 2013

Published online 9 October 2013 in Wiley Online Library (wileyonlinelibrary.com).

DOI: 10.1002/prot.24443

development of resistance to drugs used for the treatment of cancers.<sup>2–4</sup> Specifically, anamorsin has been shown to play a role in conferring multidrug resistance to gastric cancer cells by upregulating multidrug resistance gene-1 (MDR-1) and multidrug related protein-1 (MRP-1) expression.<sup>5</sup> Studies on cellular localization have revealed that anamorsin is found in the cytoplasm as well as nucleus of both human and mouse cells.<sup>6</sup> Anamorsin is expressed ubiquitously in various tissues and its expression is induced by various cytokines through the Ras signaling pathway, suggesting that it might be performing an important conserved function, details of which are currently not known.<sup>1,7</sup> Human anamorsin shares 82% amino acid sequence identity with its homolog from mouse. On the other hand, the yeast homolog of anamorsin named Dre2 shares only 12% sequence identity and was originally identified as a Fe/S cluster protein.<sup>8</sup> It localizes to the cytoplasm and mitochondria, but the nucleus was not specifically examined. The C-terminal sequence, including the cysteine motifs, CX2CXC and CX2C, is highly conserved between yeast Dre2 and human anamorsin. In contrast, the N-terminal putative methyltransferase motif is not conserved. The human homolog was able to correct the lethality of yeast Dre2 deletion and it could also replace Dre2 for binding with Tah18,<sup>8,9</sup> indicating that the two proteins share a common function. Both anamorsin and Dre2 have been shown to possess Fe-S cluster, and this module is important for the function of the proteins, particularly in the biogenesis of Fe-S proteins.<sup>10,11</sup>

A search for conserved domains revealed that the human anamorsin contains a methyltransferase motif at the N-terminal. Interestingly, this motif was not detected by the conserved domain search in Dre2. However, a recent NMR structure of a truncation of the Dre2 N-terminus shows a partial S-adenosylmethionine methyltransferase (SAM) fold, with two  $\alpha$ -helices and a  $\beta$ -strand missing from the SAM fold.<sup>11</sup> Although anamorsin is predicted to have an S-adenosyl-L-methionine (AdoMet) dependent methyltransferase activity, experimental data is needed to substantiate the prediction. Initial studies on AdoMet dependant methyltransferase activity of purified anamorsin have revealed that it does not possess any measurable DNA or RNA methyltransferase activity.<sup>12</sup> To find out why anamorsin does not show methyltransferase activity and to obtain clues on the function of the protein, we decide to obtain a structural view of anamorsin. Here, we report the crystal structure of the N-terminal putative methyltransferase domain. Comparison of the structure with other methyltransferases reveals differences in the AdoMet-binding pocket that prevents the N-terminal domain of anamorsin from binding AdoMet. Therefore, anamorsin is incapable of AdoMet-based methyltransfers.

## METHODS

### Protein expression and purification

A 939-base pair DNA fragment coding human anamorsin (NP\_064709) was amplified using forward primer: 5'-TACTTCCAATCCAATGCTATGGCAGATTTTGG-3' and reverse primer: 5'-TTATCCACTTCCAATGCTAGGCATCATGAAGA-3', respectively. The resulting DNA fragment was ligated into vector pMCSG7<sup>13</sup> using ligase-independent cloning and transformed into *E. coli* BL21(DE3) cells. The cells were cultured at 37°C in Luria-Bertani (LB) medium containing 100  $\mu$ g/mL ampicillin until OD<sub>600nm</sub> = 0.8, after which the cells were induced with 0.2 mM isopropyl-*b*-D-thiogalactoside (IPTG) at 16°C overnight. The cells were harvested by centrifugation at 4000 rpm/min, suspended in phosphate-buffered saline (PBS) (137 mM NaCl, 2.7 mM KCl, 50 mM Na<sub>2</sub>HPO<sub>4</sub>, 10 mM KH<sub>2</sub>PO<sub>4</sub>, pH 7.4) and stored at –20°C until further use.

The protein was purified as described before.<sup>14</sup> Briefly, cell pellets were lysed by sonication and the supernatant was loaded onto a Ni-NTA column (Qiagen) equilibrated with PBS. After washing with 100 mL of binding buffer (PBS) followed by 50 mL of washing buffer (PBS containing 20 mM imidazole), the fusion protein was eluted with 10 mL of elution buffer (PBS containing 300 mM imidazole). The purified protein was then concentrated and loaded on Superdex G75 size exclusion chromatography column (Amersham) equilibrated with 20 mM Tris-HCl, pH 8.0, and 200 mM NaCl. Fractions containing the protein were pooled, concentrated, and stored at –20°C.

Full-length anamorsin degraded during purification and it was hard to obtain homogeneous protein prep. Therefore, we performed limited proteolysis using chymotrypsin to obtain a stable fragment. A combination of mass spectrometry and N-terminal sequencing identified the fragment as the N-terminal (AA 1–172) region of anamorsin. This region was re-cloned and the fragment of anamorsin was expressed and purified using *E. coli* following the same procedure as that described before for the full-length protein. The purified protein was concentrated to 12 mg/mL before setting up crystallization.

### Crystallization and data collection

Anamorsin (AA 1–172) was screened for crystallization using the hanging drop vapor diffusion method. Each 2  $\mu$ L drop contained equal volumes of protein and reservoir solution. After a week, crystals of anamorsin (AA 1–172) grew at 16°C in a condition containing 0.17M sodium acetate trihydrate, 0.085M sodium cacodylate pH6.5, 25% polyethylene glycol 8000, 15% Glycerol. Single crystals were frozen in liquid nitrogen prior to X-ray diffraction testing and data collection. Native data were collected at a wavelength of 1.5418 Å on a copper

**Table I**  
Data Collection and Refinement Statistics<sup>a</sup>

	Native	Hg derivative
Data		
Space group	$P6_1$	$P6_1$
Cell dimensions		
$a, b, c$ (Å)	79.43, 79.43, 101.56	79.51, 79.51, 101.75
$\alpha, \beta, \gamma$ (°)	90.00, 90.00, 120.00	90.00, 90.00, 120.00
Resolution (Å)	50.00–2.30 (2.34–2.30)	50.00–1.80 (1.83–1.80)
$R_{\text{sym}}^b$	0.084 (0.425)	0.067 (0.51)
$I/\sigma I$	31.16 (3.01)	42.9 (4.09)
Completeness (%)	100.0 (99.6)	100.0 (100.0)
Redundancy	9.9 (4.6)	10.7 (7.5)
Refinement		
Resolution (Å)		30.43–1.80
No. reflections		33,703
$R_{\text{work}}/R_{\text{free}}^c$		18.5/22.4
R.m.s deviations		
Bond lengths (Å)		0.007
Bond angles (°)		1.03
Residue range		
Ramachandran <sup>d</sup> (%)		98.4/1.6/0
PDB code		4M7R

<sup>a</sup>Values for highest resolution shells are in parentheses.

<sup>b</sup> $R_{\text{sym}} = \sum_i |h|I(i, h) - \langle I(h) \rangle / \sum_i |h|I(i, h)$  where  $I(i, h)$  and  $\langle I(h) \rangle$  are the  $i$ th and mean measurement of intensity of reflection  $h$ .

<sup>c</sup> $R_{\text{free}}$  was calculated using 5% of the data.

<sup>d</sup>Residues in favored, accepted, and outlier regions of the Ramachandran plot as reported by MOLPROBITY.

rotating anode X-ray source and R-Axis IV11 detector (Rigaku). During the data collection, the crystal was maintained at 100 K using nitrogen gas. Crystals soaked in  $(\text{C}_2\text{H}_5\text{HgO})\text{HPO}_2$  for 2 h were used for heavy atom derivatization and the data were collected at a wavelength of 1.0000 Å at beamline 19-ID, Advanced Photon Source, Argonne National Laboratory. The diffraction data were

processed with the HKL2000 suite of program.<sup>15</sup> Both native and derivative crystals belong to space group  $P6_1$ . Details of data collection statistics are listed Table I.

## Structure determination

The structure was solved by Single wavelength Anomalous Diffraction method. SOLVE<sup>16</sup> was used to search and localize the positions of Hg atoms. The initial model and phases were obtained using OASIS.autobuild. The model was refined manually in Coot<sup>17</sup> and automatically in PHENIX.<sup>18</sup> The  $R_{\text{work}}$  and  $R_{\text{free}}$  values of the final model are 0.18 and 0.22, respectively. The stereochemical analysis of the final model was performed by MOLPROBITY.<sup>19</sup> Refinement statistics and geometry are presented in Table I.

## RESULTS AND DISCUSSION

## Overall structure of the N-terminal domain of anamorsin

Full-length anamorsin expressed and purified from *E. coli* did not crystallize. Therefore, we subjected the protein to limited proteolysis. A stable fragment of anamorsin was identified using chymotrypsin. N-terminal amino acid sequencing results coupled with MS data revealed that the fragment consisted of the N-terminal 1–172 residues [Fig. 1(A)]. This N-terminal fragment was recloned and expressed in *E. coli*. After purification, the truncated anamorsin crystallized readily. The structure of the N-terminal fragment was solved to 1.8 Å resolution. Phases were calculated using data collected from Hg compound soaked crystals.

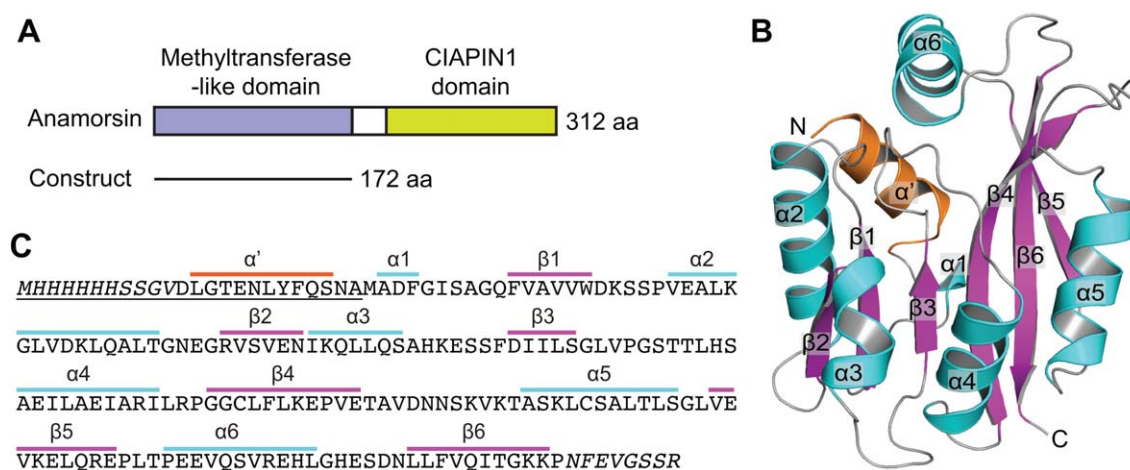


### Figure 1

Crystal structure of anamorsin N-terminal methyltransferase-like domain. **A:** Domain organization of anamorsin and the construct used for crystallization. **B:** A cartoon representation of the methyltransferase-like domain. The helices and sheets are colored cyan and magenta respectively, except  $\alpha'$  derived from the vector is in yellow. **C:** Primary sequence of N-terminal domain annotated with secondary structural elements. Residues originating from the expression vector are underlined.

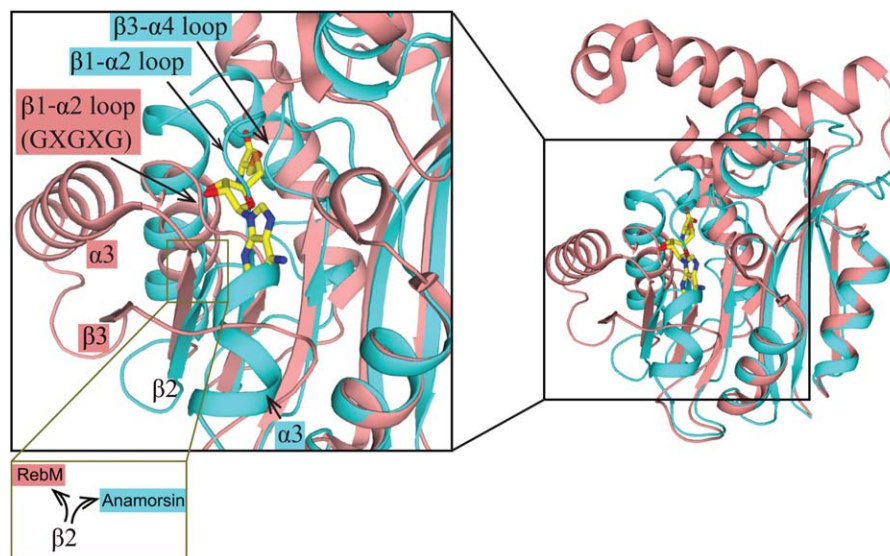


**Figure 2**

Anamorsin shows features that are distinct from the SAM-dependant methyltransferase RebM. The methyltransferase domain of RebM (PDB code 3BUS) was superimposed over the structure of the N-terminal region of anamorsin. In the RebM structure, SAM is depicted as stick, the  $\alpha 3$ - $\beta 3$  elements that not present in anamorsin structure are labeled;  $\beta 1$ - $\alpha 2$  loop bearing the SAM-binding GxGxG motif is marked. In anamorsin, the  $\alpha 3$ -helix,  $\beta 1$ - $\alpha 2$  loop, and  $\beta 3$ - $\alpha 4$  loop that otherwise will clash with SAM are indicated by arrows.

The asymmetric unit consists of a dimer of the protein based on the calculated solvent content of 51%. However, the size exclusion chromatography profile of anamorsin and PISA analysis suggested that the fragment exists as a monomer. Except for a few residues like F168-R172 (F192-R196, if includes the 24-residues tag) of chain A and N165-R172 (N189-R196, if includes the 24-residues tag) of chain B, electron density for most of the polypeptide was of good quality. Residues 12–24 of the tag form a  $\alpha$ -helix at the N-terminus ( $\alpha'$ ). In one asymmetric unit, only one Hg covalently binds to the side chain of C116 in chain A with a lower occupancy (30%), and the Hg derivation does not induce any significant difference between the two chains.

The N-terminal of anamorsin folds into a Rossmann-like fold with  $\alpha/\beta$  topology [Fig. 1(B,C)]. Six strands, in the order  $\beta 2$ ,  $\beta 1$ ,  $\beta 3$ ,  $\beta 4$ ,  $\beta 6$ , and  $\beta 5$ , form a central twisted sheet. While strands  $\beta 1$ – $\beta 5$  run parallel,  $\beta 6$  is positioned anti-parallel. The sheet is flanked by three helices on each side. A search of the Protein Data Bank for structural homologues of anamorsin using DALI<sup>20</sup> revealed that the N-terminus of anamorsin is similar in structure to methyl transferases. The best match was a SAM-dependant rebeccamycin 4'-O-methyltransferase, RebM, (PDB code 3BUS, Z score of 13.2, overlap of 145 residues out of a total of 172 residues of truncated anamorsin with an rmsd of 2.6 Å and 23% sequence identity) (Fig. 2) followed by SAM bound YcgJ protein (PDB code 2glu, Z score of 12.9, overlap of 142 residues out of a total of 172 residues of truncated anamorsin with a

rmsd of 3.1 Å and 18% sequence identity). Thus, the N-terminus of anamorsin is reminiscent of the SAM-dependant methyltransferase domain.

#### Anamorsin shows no detectable methyltransferase activity

The N-terminal region of anamorsin is structurally similar to methyl transferases. A previous study showed that insect cells expressed anamorsin failed to methylate or demethylate DNA or RNA.<sup>12</sup> Using similar way, we further found that the full-length and truncated anamorsin purified from *E. coli* and mammalian cells showed no SAM dependant methyltransferase activity when compared to the positive control assayed under identical conditions. Several features of the structure solved by us help explain why anamorsin may not be able to catalyze SAM-dependant methyl transfers in spite of sharing structural motifs very similar to methyl transferases (Fig. 2). First, the conserved signature motif, GxGxG, used by methyltransferases to bind SAM is not present in anamorsin. Second, the central sheet of anamorsin is made up of six strands as opposed to seven or eight strands observed in most methyltransferases. Superimposition of the structure of the methyltransferase RebM over the structure of anamorsin reveals that the  $\beta 3$ - $\alpha 3$  structural elements observed near the SAM binding pocket of RebM are missing in anamorsin. Instead, the C-terminus of  $\beta 2$  of anamorsin flips in opposite direction forming a new short helix ( $\alpha 3$ ) that further constricts the SAM binding pocket.



Lastly, when compared to other methyltransferases, the  $\alpha 2$ -helix, seen in the vicinity of the SAM-binding pocket, is much longer in the structure of anamorsin. This results in the  $\beta 1$ - $\alpha 2$  loop (SAM binding loop) sterically blocking the SAM binding pocket. Similarly, an unusually longer  $\beta 3$ - $\alpha 4$  loop imposes further restrictions on accessing the SAM binding pocket. These structural features prevent binding of SAM to anamorsin (Fig. 2). In fact, addition of SAM in buffers during purification of the protein or soaking of anamorsin crystals with SAM did not reveal any density for the ligand, further confirming the structural observations that anamorsin cannot bind SAM. Taken together, these results indicate that anamorsin might have either lost its ability to bind SAM and carry out methyl transfers or may have evolved to carry out a new function using the methyltransferase fold.

Several recent references showed that anamorsin and its ortholog in yeast, Dre2, play a functional role in the cytosolic Fe/S cluster maturation pathway.<sup>10,21</sup> Anamorsin and NADPH-dependent diflavin oxidoreductase 1 (Ndr1) form a stable complex that can functionally replace the Dre2-Tah18 complex in yeast cells.<sup>9,21,22</sup> The function of anamorsin relies on the [2Fe-2S] cluster in the CIAPIN1 domain that receives one electron transferred from the FMN moiety of Ndr1.<sup>23</sup> Anamorsin-Ndr1 complex is also suggested to be critical for the regulation of cell survival/death by monitoring the intracellular redox status.<sup>21–23</sup> The Ndr1-binding region in anamorsin, however, is specified to the middle nonstructured linker region and the C-terminal Fe-S containing CIAPIN1 domain.<sup>23</sup> Therefore, how the N-terminal methyltransferase-like domain is involved in these functions is still elusive. It is possible that the methyltransferase-like domain contributes as a scaffold for the function of CIAPIN1 domain, or it may be involved in other protein:protein interaction. For example, the PKC $\theta$  interacting cousin of thioredoxin, PICOT, was shown to bind the N-terminal region of anamorsin by yeast-two-hybrid assay.<sup>24</sup> Interestingly, the PICOT is also a Fe-S cluster protein.<sup>25</sup> So presumably the methyltransferase-like domain in anamorsin function as an adaptor in the cytosolic iron-sulfur protein assembly machinery. A structure of the complex of anamorsin with PICOT is likely to shed light on the exact function of the methyltransferase-like domain of anamorsin.

## ACKNOWLEDGMENTS

Crystallographic data were collected at 19-ID beamline at the Advanced Photon Source, Argonne National Laboratory. Authors thank Prof. Rongguang Zhang for help with data collection.

## ACCESSION CODES

Atomic coordinates and structure factors for the N-terminal domain of anamorsin are deposited in

the Protein Data Bank, [www.pdb.org](http://www.pdb.org) (PDB ID code 4M7R).

## REFERENCES

- Shibayama H, Takai E, Matsumura I, Kouno M, Morii E, Kitamura Y, Takeda J, Kanakura Y. Identification of a cytokine-induced antiapoptosis molecule anamorsin essential for definitive hematopoiesis. *J Exp Med* 2004;199:581–592.
- Zhao Y, Han Y, Liu F, An H, Shi Y, Yu Q, Fan D. Differentially expressed gene profiles between multidrug resistant gastric adenocarcinoma cells and their parental cells. *Cancer Lett* 2002;185:211–218.
- Hao Z, Qiao T, Jin X, Li X, Gao J, Fan D. Preparation and characterization of a specific monoclonal antibody against CIAPIN1. *Hybridoma* 2005;24:141–145.
- Li X, Wu K, Fan D. CIAPIN1 as a therapeutic target in cancer. *Expert Opin Ther Targets* 2010;14:603–610.
- Hao Z, Li X, Qiao T, Du R, Hong L, Fan D. CIAPIN1 confers multidrug resistance by upregulating the expression of MDR-1 and MRP-1 in gastric cancer cells. *Cancer Biol Ther* 2006;5:261–266.
- Hao Z, Li X, Qiao T, Du R, Zhang G, Fan D. Subcellular localization of CIAPIN1. *Histochem Cytochem* 2006;54:1437–1444.
- Hao Z, Li X, Qiao T, Zhang J, Shao X, Fan D. Distribution of CIAPIN1 in normal fetal and adult human tissues. *J Histochem Cytochem* 2006;54:417–426.
- Zhang Y, Lyver ER, Nakamaru-Ogiso E, Yoon H, Amutha B. Dre2, a conserved eukaryotic Fe/S cluster protein, functions in cytosolic Fe/S protein biogenesis. *Mol Cell Biol* 2008;28:5569–5582.
- Vernis L, Facca C, Delagoutte E, Soler N, Chanet R, Guiard B, Faye G, Baldacci G. A newly identified essential complex, Dre2-Tah18, controls mitochondria integrity and cell death after oxidative stress in yeast. *PLoS One* 2009;4:4376–4389.
- Banci L, Bertini I, Ciofi-Baffoni S, Boscaro F, Chatzi A, Mikolajczyk M, Tokatlidis K, Winkelmann J. Anamorsin is a [2Fe-2S] cluster-containing substrate of the Mia40-dependent mitochondrial protein trapping machinery. *Chem Biol* 2011;18:794–804.
- Soler N, Craescu CT, Gallay J, Frapart Y, Mansuy D, Raynal B, Baldacci G, Pastore A, Huang ME, Vernis L. A S-adenosylmethionine methyltransferase-like domain within the essential, Fe-S-containing yeast protein Dre2. *FEBS J* 2012;279:2108–2119.
- Hao Z, Li X, Qiao T, Fan D. Successful expression and purification of human CIAPIN1 in baculovirus-insect cell system and application of this system to investigation of its potential methyltransferase activity. *Int J Biol Macromol* 2008;42:27–32.
- Stols L, Gu M, Dieckman L, Raffin R, Collart FR, Donnelly MI. A new vector for high-throughput, ligation-independent cloning encoding a tobacco etch virus protease cleavage site. *Protein Expr Purif* 2002;25:8–15.
- Song G, Li Y, Cheng C, Zhao Y, Gao A, Zhang R, Joachimiak A, Shaw N, Liu ZJ. Structural insight into acute intermittent porphyria. *FASEB J* 2009;23:396–404.
- Otwinski Z, Minor W. Processing of X-ray diffraction data collected in oscillation mode. *Methods Enzymol* 1997;276:307–326.
- Terwilliger TC, Berendzen J. Automated MAD and MIR structure solution. *Acta Crystallogr D* 1999;55:849–861.
- Emsley P, Cowtan K. Coot: model-building tools for molecular graphics. *Acta Crystallogr D* 2004;60:2126–2132.
- Adams PD, Afonine PV, Bunkóczi G, Chen VB, Davis IW, Echols N, Headd JJ, Hung LW, Kapral GJ, Grosse-Kunstleve RW, McCoy AJ, Moriarty NW, Oeffner R, Read RJ, Richardson DC, Richardson JS, Terwilliger TC, Zwart PH. PHENIX: a comprehensive Python-based system for macromolecular structure solution. *Acta Crystallogr D* 2010;66 (Part 2):213–221.
- Davis IW, Leaver-Fay A, Chen VB, Block JN, Kapral GJ, Wang X, Murray LW, Arendall WB III, Snoeyink J, Richardson JS, Richardson DC. MolProbity: all-atom contacts and structure

- validation for proteins and nucleic acids. *Nucleic Acids Res* 2007;35:W375–W383.
20. Holm L, Rosenström P. Dali server: conservation mapping in 3D. *Nucleic Acids Res* 2010;38:W545–W549.
  21. Netz DJ, Stumpfig M, Dore C, Muhlenhoff U, Pierik AJ, Lill R. Tah18 transfers electrons to Dre2 in cytosolic iron-sulfur protein biogenesis. *Nat Chem Biol* 2010;6:758–765.
  22. Soler N, Delagoutte E, Miron S, Facca C, Baille D, D'Autreaux B, Craescu G, Frapart YM, Mansuy D, Baldacci G, Huang ME, Vernis L. Interaction between the reductase Tah18 and highly conserved Fe-S containing Dre2 C-terminus is essential for yeast viability. *Mol Microbiol* 2011;82:54–67.
  23. Banci L, Bertini I, Calderone V, Ciofi-Baffoni S, Giachetti A, Jaiswal D, Mikolajczyk M, Piccoli M, Winkelmann J. Molecular view of an electron transfer process essential for iron–sulfur protein biogenesis. *Proc Natl Acad Sci USA* 2013;110:7136–7141.
  24. Saito Y, Shibayama H, Tanaka H, Tanimura A, Matsumura I, Kanakura Y. PICOT is a molecule which binds to anamorsin. *Biochem Biophys Res Commun* 2011;408:329–333.
  25. Haunhorst P, Berndt C, Eitner S, Godoy JR, Lillig CH. Characterization of the human monothiol glutaredoxin 3 (PICOT) as iron–sulfur protein. *Biochem Biophys Res Commun* 2010;394:372–376.